

# System Parameters Evaluation of Flexibly Supported Laminated Composite Sandwich Plates

C. R. Lee,\* S. J. Sun,\* and T. Y. Kam†

*National Chiao Tung University, Hsin Chu 300, Taiwan, Republic of China*

DOI: 10.2514/1.23598

**A nondestructive evaluation technique established on the basis of a global minimization method is presented for the system parameters identification of flexibly supported rectangular laminated composite sandwich plates using measured natural frequencies of the sandwich plates. In this study, the first eight natural frequencies extracted from impulsive vibration testing data are used to identify the system parameters of the flexibly supported sandwich plates. In the identification process, the trial system parameters are used in the Rayleigh–Ritz method to predict the theoretical natural frequencies of the sandwich plate, a frequency discrepancy function is established to measure the sum of the squared differences between the experimental and theoretical predictions of the natural frequencies, and the global minimization method is used to search for the best estimates of the system parameters by making the frequency discrepancy function a global minimum. The accuracy and efficiency of the proposed technique in identifying the system parameters of several flexibly supported sandwich plates made of different face and core materials are studied via both theoretical and experimental approaches. The reasonably good results obtained in this study have demonstrated the applicability of the proposed technique.**

## I. Introduction

**B**ECAUSE of their high strength/stiffness to weight ratios, fiber reinforced composite sandwich plates have been widely used in the aerospace industry to fabricate high performance structures. In general, the composite sandwich plates in these structures are connected to other members using different joining methods. One popular way to analyze the mechanical behaviors of the composite sandwich plates is to consider the plates being supported at the boundary by equivalent elastic restraints. The attainment of the actual behavioral predictions of the flexibly supported composite sandwich plates, however, depends on the correctness of the system parameters such as the elastic constants of the plates and the spring constants of the elastic restraints at the plate boundaries. As is well known, composite structures fabricated using different methods or curing processes may possess different mechanical properties, and because of this the material properties determined from the standard specimens tested in the laboratory in general may deviate from those of the actual laminated composite structures. Furthermore when in service, the material properties of composite structures may degrade due to aging or environmental effects. Because the attainment of actual system parameters is vital to the integrity assessment of structures, the determination of the mechanical properties of structures, especially composite plate structures, has thus become an important topic of research in recent years. For instance, Deobald and Gibson [1] used a Rayleigh–Ritz/modal analysis technique to determine the elastic constants of composite plates with different boundary conditions. Castagnède et al. [2] determined the elastic constants of thick composite plates via a quantitative ultrasonic approach. Fallstrom and Jonsson [3] determined the material constants of anisotropic plates from the frequencies and mode shapes measured by a real-time TV-holography system. Several researchers [4–6] developed methods to identify structural stiffness matrices or the element bending stiffness of beam structures using measured natural frequencies and mode shapes. Wang and Kam [7] developed

a two-stage nondestructive evaluation method in which strains and/or displacements obtained from static testing of laminated composite plates clamped at the edges are used to identify the elastic constants of the plates. Recently a number of researchers [8–11] have used experimental natural frequencies to identify the elastic constants of laminated composite plates with free boundary conditions. For instance, Moussu and Nivoit [8] used the method of superposition to determine the elastic constants of free orthotropic plates from measured natural frequencies. Sol et al. [9] used the method of Bayesian estimation to study the identification of elastic constants from the experimental natural frequencies of free rectangular orthotropic plates. Regarding the system parameters identification of sandwich plates, though it is an important topic of research, only limited work has been devoted to this area. For instance, Thwaites and Clark [12] used elastic waves to detect and identify core damage and skin delamination of honeycomb sandwich plates. Saito et al. [13] presented a method established on the basis of Timoshenko beam theory to deal with parameters identification of aluminum honeycomb sandwich panels. It is worth noting that all the structures used in the aforementioned system identification studies had regular boundary conditions such as free, clamped, simply supported ends/edges. Recently the authors have presented a method to determine the mechanical properties of laminated composite plates partially restrained by elastic supports at the plate edges using measured natural frequencies [14]. In their study, several natural frequencies extracted from measured vibration test data have been used to determine the mechanical properties of the composite plates and elastic edge restraints. Regarding the system parameters determination of laminated composite sandwich plates with elastic restraints, it seems not much attention has been drawn to this area which, however, needs to be explored in depth.

In this paper, a nondestructive evaluation method for the system parameters identification of flexibly supported laminated composite sandwich plates using measured natural frequencies is presented. In the proposed nondestructive evaluation method, the Rayleigh–Ritz method constructed on the basis of the layerwise linear displacement theory is used to predict the theoretical natural frequencies of laminated composite sandwich plates with different boundary conditions using trial system parameters. Vibration testing of flexibly supported laminated composite sandwich plates is performed to measure the natural frequencies of the plates. A frequency discrepancy function is established to measure the sum of the squared differences between the experimental and theoretical natural frequencies of the sandwich plate. The identification of the

Received 3 March 2006; accepted for publication 2 May 2007. Copyright © 2007 by the American Institute of Aeronautics and Astronautics, Inc. All rights reserved. Copies of this paper may be made for personal or internal use, on condition that the copier pay the \$10.00 per-copy fee to the Copyright Clearance Center, Inc., 222 Rosewood Drive, Danvers, MA 01923; include the code 0001-1452/07 \$10.00 in correspondence with the CCC.

\*Research Assistant, Department of Mechanical Engineering.

†Professor, Department of Mechanical Engineering; tykam@mail.nctu.edu.tw. Member AIAA (Corresponding Author).

system parameters of the sandwich plate is then formulated as a constrained minimization problem in which the system parameters are determined by making the frequency discrepancy function a global minimum. The capability and efficiency of the proposed method in identifying accurate system parameters of laminated composite sandwich plates with different properties will be demonstrated by means of a number of examples.

## II. Vibration Analysis of Composite Sandwich Plate

Without loss of generality, consider the elastically restrained rectangular symmetric composite sandwich plate of area  $a \times b$  and constant thickness  $h$  composed of two same thin laminated composite sheets with thicknesses  $h_f$  at the top and bottom surfaces of the relatively thick core layer with thickness  $h_c$  as shown in Fig. 1. The  $x$  and  $y$  coordinates of the plate are taken in the midplane of the plate. It is assumed that the edge flexible supports of the plate can be modeled by longitudinal and torsional springs as shown in Fig. 2. Herein the layerwise linear displacement theory [15,16] is used to determine the displacement field of the sandwich plate. The sandwich plate is divided into three layer groups in which the core, upper face sheet, and lower face sheet are numbered as layer groups 1, 2, and 3, respectively. The displacement components of the sandwich plate are assumed to be of the following forms.

$$\begin{aligned} w_0(x, y, t) &= W(x, y) \sin \omega t \\ \theta_x^{(k)}(x, y, t) &= \Theta_x^{(k)}(x, y) \sin \omega t \quad k = 1 \sim 3 \\ \theta_y^{(k)}(x, y, t) &= \Theta_y^{(k)}(x, y) \sin \omega t \end{aligned} \quad (1)$$

where  $w_0(x, y, t)$  is vertical deflection at plate midplane;  $\theta_x^{(k)}(x, y, t)$  and  $\theta_y^{(k)}(x, y, t)$  are rotations of the cross sections perpendicular to  $x$  and  $y$  axes, respectively, of the  $k$ th layer group;  $W$  is deflection function;  $\Theta_x^{(k)}$  and  $\Theta_y^{(k)}$  are rotation functions;  $\omega$  is angular frequency;  $t$  is time. In view of Fig. 3, the displacement field of the core (layer group 1) is given as

$$\begin{aligned} u^{(1)}(x, y, z, t) &= u_0(x, y, t) + \xi^{(1)} \theta_x^{(1)}(x, y, t) \\ v^{(1)}(x, y, z, t) &= v_0(x, y, t) + \xi^{(1)} \theta_y^{(1)}(x, y, t) \\ w^{(1)}(x, y, z, t) &= w_0(x, y, t) \end{aligned} \quad (2)$$

where  $u^{(1)}$  and  $v^{(1)}$  are in-plane displacements at any point in  $x$  and  $y$

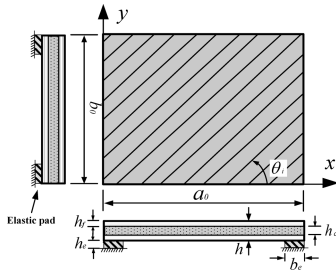


Fig. 1 Flexibly supported composite sandwich plate.

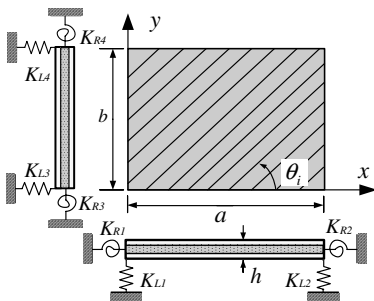


Fig. 2 Mathematical model of flexibly supported sandwich plate.

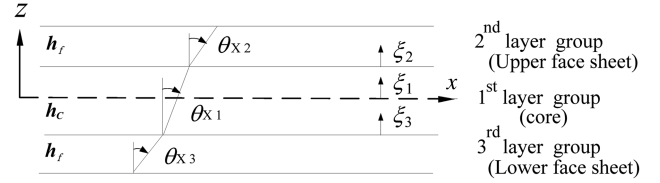


Fig. 3 Layer groups of laminated composite sandwich plate.

directions, respectively;  $u_0$ ,  $v_0$  are in-plane displacements at the midplane;  $w^{(1)}$  is vertical displacement in the  $z$  direction;  $\xi^{(1)}$  is the local coordinate in the thickness direction.

Similarly the displacement fields of the upper face sheet (layer group 2) and lower face sheet (layer group 3) are given, respectively, as follows: Upper face sheet

$$\begin{aligned} u^{(2)}(x, y, z, t) &= u^{(1)}\left(x, y, \frac{h_c}{2}, t\right) + \xi^{(2)} \theta_x^{(2)}(x, y, t) \\ v^{(2)}(x, y, z, t) &= v^{(1)}\left(x, y, \frac{h_c}{2}, t\right) + \xi^{(2)} \theta_y^{(2)}(x, y, t) \\ w^{(2)}(x, y, z, t) &= w_0(x, y, t) \end{aligned} \quad (3a)$$

Lower face sheet

$$\begin{aligned} u^{(3)}(x, y, z, t) &= u^{(1)}\left(x, y, -\frac{h_c}{2}, t\right) + \xi^{(3)} \theta_x^{(3)}(x, y, t) \\ v^{(3)}(x, y, z, t) &= v^{(1)}\left(x, y, -\frac{h_c}{2}, t\right) + \xi^{(3)} \theta_y^{(3)}(x, y, t) \\ w^{(3)}(x, y, z, t) &= w_0(x, y, t) \end{aligned} \quad (3b)$$

where  $\xi^{(k)}$  is a local coordinate in the  $k$ th layer group. It is noted that for small deflection,  $u_0$  and  $v_0$  are negligible and thus can be discarded. Therefore seven independent displacement components are left for the sandwich plates with elastically restrained edges. The strain-displacement relations for each layer group can be expressed in matrix form as

$$\begin{Bmatrix} \varepsilon_x^{(k)} \\ \varepsilon_y^{(k)} \\ \gamma_{xy}^{(k)} \\ \gamma_{yz}^{(k)} \\ \gamma_{xz}^{(k)} \end{Bmatrix} = \begin{Bmatrix} \frac{\partial u^{(k)}}{\partial x} \\ \frac{\partial v^{(k)}}{\partial y} \\ \frac{\partial u^{(k)}}{\partial y} + \frac{\partial v^{(k)}}{\partial x} \\ \frac{\partial v^{(k)}}{\partial z} + \frac{\partial w^{(k)}}{\partial y} \\ \frac{\partial u^{(k)}}{\partial z} + \frac{\partial w^{(k)}}{\partial x} \end{Bmatrix} \quad (4)$$

where  $\varepsilon$ ,  $\gamma$  are normal and shear strains, respectively; the superscript  $(k)$  denotes layer group number. The stress-strain relations for the three layer groups in the global  $x$ - $y$ - $z$  coordinate system can be expressed in the following general form [17]:

$$\begin{Bmatrix} \sigma_{xm}^{(k)} \\ \sigma_{ym}^{(k)} \\ \tau_{xym}^{(k)} \\ \tau_{yzm}^{(k)} \\ \tau_{xzm}^{(k)} \end{Bmatrix} = \begin{bmatrix} \bar{Q}_{11m}^{(k)} & \bar{Q}_{12m}^{(k)} & \bar{Q}_{16m}^{(k)} & 0 & 0 \\ \bar{Q}_{12m}^{(k)} & \bar{Q}_{22m}^{(k)} & \bar{Q}_{26m}^{(k)} & 0 & 0 \\ \bar{Q}_{16m}^{(k)} & \bar{Q}_{26m}^{(k)} & \bar{Q}_{66m}^{(k)} & 0 & 0 \\ 0 & 0 & 0 & \bar{Q}_{44m}^{(k)} & \bar{Q}_{45m}^{(k)} \\ 0 & 0 & 0 & \bar{Q}_{45m}^{(k)} & \bar{Q}_{55m}^{(k)} \end{bmatrix} \begin{Bmatrix} \varepsilon_{xm}^{(k)} \\ \varepsilon_{ym}^{(k)} \\ \gamma_{xym}^{(k)} \\ \gamma_{yzm}^{(k)} \\ \gamma_{xzm}^{(k)} \end{Bmatrix} \quad (5)$$

where  $\sigma$ ,  $\tau$  are normal and shear stresses, respectively;  $\bar{Q}_{ijm}^{(k)}$  are the transformed lamina stiffness coefficients which depend on the material properties and fiber orientation of the  $m$ th lamina in the  $k$ th layer group. The relations between the transformed and untransformed lamina stiffness coefficients are expressed as

$$\begin{aligned}
\bar{Q}_{11} &= Q_{11}C^4 + 2(Q_{12} + 2Q_{66})C^2S^2 + Q_{22}S^4 \\
\bar{Q}_{12} &= (Q_{11} + Q_{22} - 4Q_{66})C^2S^2 + Q_{12}(C^4 + S^4) \\
\bar{Q}_{16} &= (Q_{11} - Q_{12} - 2Q_{66})C^3S + (Q_{12} - Q_{22} + 2Q_{66})CS^3 \\
\bar{Q}_{22} &= Q_{11}S^4 + 2(Q_{12} + 2Q_{66})C^2S^2 + Q_{22}C^4 \\
\bar{Q}_{26} &= (Q_{11} - Q_{12} - 2Q_{66})CS^3 + (Q_{12} - Q_{22} + 2Q_{66})C^3S \\
\bar{Q}_{66} &= (Q_{11} + Q_{22} - 2Q_{12} - 2Q_{66})C^2S^2 + Q_{66}(C^4 + S^4) \\
\bar{Q}_{44} &= Q_{44}C^2 + Q_{55}S^2, \quad \bar{Q}_{45} = (Q_{55} - Q_{44})CS \\
\bar{Q}_{55} &= Q_{55}C^2 + Q_{44}S^2
\end{aligned} \quad (6)$$

with

$$\begin{aligned}
Q_{11} &= \frac{E_1}{1 - \nu_{12}\nu_{21}}; \quad Q_{12} = \frac{\nu_{12}E_2}{1 - \nu_{12}\nu_{21}}; \quad Q_{22} = \frac{E_2}{1 - \nu_{12}\nu_{21}} \\
Q_{44} &= G_{23}; \quad Q_{55} = G_{13}; \quad Q_{66} = G_{12} \\
C &= \cos \theta_i; \quad S = \sin \theta_i
\end{aligned} \quad (7)$$

where  $Q_{ij}$  are untransformed lamina stiffness coefficients;  $E_1, E_2$  are Young's moduli in the fiber and transverse directions, respectively;  $\nu_{ij}$  is Poisson's ratio for transverse strain in the  $j$  direction when stressed in the  $i$  direction;  $G_{12}$  is in-plane shear modulus in the 1–2 plane;  $G_{13}$  and  $G_{23}$  are transverse shear moduli in the 1–3 and 2–3 planes, respectively;  $\theta_i$  is the lamina fiber angle of the  $i$ th lamina. Herein for the thin face sheets, the transverse shear effects are assumed to be so small that the transverse shear moduli ( $G_{13}$  and  $G_{23}$ ) are treated the same as the in-plane shear modulus ( $G_{12}$ ). For the core made of isotropic material, the independent elastic constants in Eq. (7) are Young's modulus  $E_c$  and Poisson's ratio  $\nu_c$ . The strain energy  $U_p$  and kinetic energy  $T$  of the plate are expressed, respectively, as

$$U_p = \sum_{k=1}^3 \int_{V^{(k)}} \frac{1}{2} \sigma^{(k)T} \epsilon^{(k)} dV^{(k)} \quad (8)$$

and

$$T = \sum_{k=1}^3 \frac{1}{2} \int_{V^{(k)}} \rho^{(k)} (\dot{u}^{(k)2} + \dot{v}^{(k)2} + \dot{w}^{(k)2}) dV^{(k)} \quad (9)$$

where  $\rho^{(k)}$  is material density;  $V^{(k)}$  is volume;  $\sigma^{(k)T} = [\sigma_x^{(k)}, \sigma_y^{(k)}, \tau_{xy}^{(k)}, \tau_{yz}^{(k)}, \tau_{xz}^{(k)}]$ , the stress vector;  $\epsilon^{(k)T} = [\epsilon_x^{(k)}, \epsilon_y^{(k)}, \gamma_{xy}^{(k)}, \gamma_{yz}^{(k)}, \gamma_{xz}^{(k)}]$ , the strain vector, respectively;  $\dot{u}, \dot{v}$ , and  $\dot{w}$  are velocities in  $x, y$ , and  $z$  directions, respectively. After substituting the displacement equations and stress–strain relations into Eqs. (8) and (9), the maximum strain energy  $U_{pm}$  and kinetic energy  $T_m$  of the plate can be obtained by letting the terms of  $\sin \omega t$  and  $\cos \omega t$  equal to 1. For the plate restrained by elastic edge supports, additional strain energy stored in the boundary springs exists. A general form for evaluating the maximum total strain energy of the flexible restraints,  $U_B$ , is written as

$$\begin{aligned}
U_B &= \frac{K_{L1}}{2} \left[ \int_0^b W^2 dy \right]_{x=0} + \frac{K_{L2}}{2} \left[ \int_0^b W^2 dy \right]_{x=a} \\
&+ \frac{K_{L3}}{2} \left[ \int_0^a W^2 dx \right]_{y=0} + \frac{K_{L4}}{2} \left[ \int_0^a W^2 dx \right]_{y=b} \\
&+ \sum_{k=1}^3 \left\{ \frac{K_{R1}^{(k)}}{2} \left[ \int_0^b \Theta_x^{(k)2} dy \right]_{x=0} + \frac{K_{R2}^{(k)}}{2} \left[ \int_0^b \Theta_x^{(k)2} dy \right]_{x=a} \right. \\
&\left. + \frac{K_{R3}^{(k)}}{2} \left[ \int_0^a \Theta_y^{(k)2} dx \right]_{y=0} + \frac{K_{R4}^{(k)}}{2} \left[ \int_0^a \Theta_y^{(k)2} dx \right]_{y=b} \right\} \quad (10)
\end{aligned}$$

where  $K_{Li}$  ( $i = 1, \dots, 4$ ) is the longitudinal spring constant intensity of the  $i$ th edge;  $K_{Ri}^{(k)}$  is the torsional spring constant intensity at the  $k$ th layer group of the  $i$ th edge. The integrals in the brackets of the above

equation are evaluated at the four edges of the plate. The total maximum strain energy of the flexibly supported plate is then written as

$$U = U_{pm} + U_B \quad (11)$$

Based on the Rayleigh–Ritz method, the displacement functions can be expressed in the following nondimensional form:

$$\begin{aligned}
W(\xi, \eta) &= \sum_{i=1}^I \sum_{j=1}^J C_{ij}^{(1)} \phi_i^{(1)}(\xi) \varphi_j^{(1)}(\eta) \\
\Theta_x^{(k)}(\xi, \eta) &= \sum_{m=1}^M \sum_{n=1}^N C_{mn}^{(2k)} \phi_m^{(2k)}(\xi) \varphi_n^{(2k)}(\eta) \quad k = 1 \sim 3 \\
\Theta_y^{(k)}(\xi, \eta) &= \sum_{p=1}^P \sum_{q=1}^Q C_{pq}^{(2k+1)} \phi_p^{(2k+1)}(\xi) \varphi_q^{(2k+1)}(\eta)
\end{aligned} \quad (12)$$

where  $C_{pq}$  are undetermined displacement coefficients;  $\phi(\xi), \varphi(\eta)$  are the characteristic functions;  $\xi, \eta$  are normalized coordinates; the superscripts denote displacement coefficients for different layer groups. Herein the Legendre's orthogonal polynomials are used in Eq. (12) to denote  $\phi_i$  and  $\varphi_j$ . For instance,  $\phi_i(\xi)$  is written as

$$\phi_1(\xi) = 1 \quad \phi_2(\xi) = \xi$$

and for  $n \geq 3$ ,

$$\phi_n(\xi) = [(2n-3)\xi \times \phi_{n-1}(\xi) - (n-2) \times \phi_{n-2}(\xi)] / (n-1) \quad (13)$$

where  $\xi = (2x/a) - 1$  with  $-1 \leq \xi \leq 1$ , and  $\eta = (2y/b) - 1$  with  $-1 \leq \eta \leq 1$ . It is noted that the above orthogonal polynomials  $\phi_i(\xi)$  satisfy the orthogonality condition.

$$\int_{-1}^1 \phi_n(\xi) \phi_m(\xi) d\xi = \begin{cases} 0, & \text{if } n \neq m \\ 2/2n-1, & \text{if } n = m \end{cases} \quad (14)$$

Extremization of the functional  $\Pi$  which is defined as  $\Pi = U - T_m$  with respect to the displacement coefficients  $C_{pq}$  leads to the following eigenvalue problem.

$$([\mathbf{K}] - \omega^2[\mathbf{M}])\{\mathbf{C}\} = 0 \quad (15)$$

where  $\{\mathbf{C}\}$  is the vector containing all the displacement coefficients;  $[\mathbf{M}]$  and  $[\mathbf{K}]$  are, respectively, structural mass and stiffness matrices in which the terms are given in the Appendix of the sandwich plates with elastically restrained edges. The natural frequencies of laminated composite sandwich plates supported by elastic restraints at the plate edges can be determined from the above equation provided that the system parameters of the plates are available. If the actual system parameters of the sandwich plate are unknown, trial system parameters can be used to predict the theoretical natural frequencies of the plate which will then be used in the system parameters identification method as will be described in the following section to determine the actual system parameters of the sandwich plates.

### III. System Identification

In this study, without loss of generality the elastic restraints under consideration are assumed to be made of strip-type pads with cross-sectional area  $b_e \times h_e$  and Young's modulus  $E_e$  as shown in Fig. 4. The expressions for determining the translational and rotational spring constant intensities of the pad-type supports have been derived via the mechanics of materials approach in the previous study [14].

$$K_L = \frac{E_e b_e}{h_e} \quad (16a)$$

and

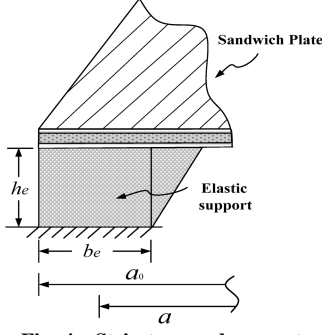


Fig. 4 Strip-type pad support.

$$K_R = \frac{E_e b_e^3}{12 h_e} \quad (16b)$$

It is noted that for a plate with length  $a_0$  and width  $b_0$  restrained by padlike edge supports, the effective length  $a$  and width  $b$  of the plate used in the Rayleigh–Ritz method become  $a_0 - \frac{b_e}{2}$  and  $b_0 - \frac{b_e}{2}$ , respectively. Herein the problem of system parameters identification of laminated composite sandwich plates restrained by strip-type pads at the plate edges is formulated as a minimization problem. In mathematical form it is stated as

$$\begin{aligned} & \text{minimize } e(\mathbf{x}) = (\boldsymbol{\omega}^*)^T (\boldsymbol{\omega}^*) \\ & \text{subject to } x_i^L \leq x_i \leq x_i^U \quad i = 1 \sim 7 \end{aligned} \quad (17)$$

where  $\mathbf{x} = [E_1, E_2, G_{12}, \nu_{12}, E_c, \nu_c, E_e]$  the vector containing the design variables which presently are system parameters of the flexibly supported composite sandwich plate;  $\boldsymbol{\omega}^*$  is an  $n \times 1$  vector containing the differences between the measured and predicted values of the natural frequencies;  $e(\mathbf{x})$  is a frequency discrepancy function measuring the sum of the squared differences between the predicted and measured data;  $x_i^L, x_i^U$  are the lower and upper bounds of the material constants. The elements in  $\boldsymbol{\omega}^*$  are expressed as

$$\omega_i^* = \frac{\omega_{pi} - \omega_{mi}}{\omega_{mi}} \quad i = 1 \sim \text{NF} \quad (18)$$

where  $\omega_{pi}, \omega_{mi}$  are predicted and measured values of the natural frequencies, respectively; NF is the number of natural frequencies. In general, the use of any conventional minimization technique to solve the identification problem of Eq. (17) may encounter great difficulty in obtaining the global minimum, that is, the actual system parameters. Herein a multistart global minimization method together with an appropriate normalization technique for normalizing the design variables is adopted to solve the above system identification problem. In the proposed method, the above problem of Eq. (17) is first converted into an unconstrained minimization problem by creating the following general augmented Lagrangian as reported in the literature [18].

$$\bar{\Psi}(\tilde{\mathbf{x}}, \boldsymbol{\mu}, \boldsymbol{\eta}, r_p) = e(\tilde{\mathbf{x}}) + \sum_{j=1}^7 \left[ \mu_j z_j + r_p z_j^2 + \eta_j \phi_j + r_p \phi_j^2 \right] \quad (19)$$

with

$$\begin{aligned} z_j &= \max \left[ g_j(\tilde{x}_j), \frac{-\mu_j}{2r_p} \right] \\ g_j(\tilde{x}_j) &= \tilde{x}_j - \tilde{x}_j^U \leq 0 \\ \phi_j &= \max \left[ H_j(\tilde{x}_j), \frac{-\eta_j}{2r_p} \right] \\ H_j(\tilde{x}_j) &= \tilde{x}_j^L - \tilde{x}_j \leq 0 \quad j = 1 \sim 7 \end{aligned} \quad (20)$$

where  $\mu_j, \eta_j, \gamma_p$  are multipliers;  $\max[0000^*, 0000^*]$  takes on the maximum value of the numbers in the bracket. The modified design variables  $\tilde{\mathbf{x}}$  are defined as

$$\tilde{\mathbf{x}} = \left[ \frac{E_1}{\alpha_1}, \frac{E_2}{\alpha_2}, \frac{G_{12}}{\alpha_3}, \frac{\nu_{12}}{\alpha_4}, \frac{E_c}{\alpha_5}, \frac{\nu_c}{\alpha_6}, \frac{E_e}{\alpha_7} \right] \quad (21)$$

where  $\alpha_i$  are normalization factors. It is noted that the choice of proper values of the normalization factors can produce appropriate search directions during the minimization process and thus help expedite the convergence of the solution. A detailed study has shown that the suitable values of  $\tilde{x}_i$  ( $i = 1, \dots, 7$ ) are better greater than 0 and less than 10. Furthermore it is worth pointing out that the original design variables are used in the Rayleigh–Ritz method to compute the theoretical natural frequencies for determining the frequency discrepancy function in Eq. (19). The update formulas for the multipliers  $\mu_j, \eta_j$ , and  $\gamma_p$  are

$$\begin{aligned} \mu_j^{n+1} &= \mu_j^n + 2r_p^n z_j^n \\ \eta_j^{n+1} &= \eta_j^n + 2r_p^n \phi_j^n \quad j = 17r_p^{n+1} \\ r_p^{n+1} &= \begin{cases} \gamma_0 r_p^n & \text{if } r_p^{n+1} < r_p^{\max} \\ r_p^{\max} & \text{if } r_p^{n+1} \geq r_p^{\max} \end{cases} \end{aligned} \quad (22)$$

where the superscript  $n$  denotes iteration number;  $\gamma_0$  is a constant;  $r_p^{\max}$  is the maximum value of  $r_p$ . Following the guideline given in the literature [18], the parameters  $\mu_j^0, \eta_j^0, r_p^0, \gamma_0, r_p^{\max}$  are chosen as

$$\mu_j^0 = 1.0 \quad \eta_j^0 = 1.0 \quad r_p^0 = 0.4 \quad \gamma_0 = 2.5 \quad r_p^{\max} = 100 \quad (23)$$

The constrained minimization problem of Eq. (17) has thus become the solution of the following unconstrained optimization problem.

Minimize

$$\text{minimize } \bar{\Psi}(\tilde{\mathbf{x}}, \boldsymbol{\mu}, \boldsymbol{\eta}, r_p) \quad (24)$$

The above unconstrained optimization problem is to be solved using the previously proposed multistart global optimization algorithm [19] which has proved to be able to locate the global minima of unconstrained minimization problems consisting of multiple local minima. In the adopted optimization algorithm, the objective function is treated as the potential energy of a traveling particle and the search trajectories for locating the global minimum are derived from the equation of motion of the particle in a conservative force field. The design variables, that is, the plate elastic constants and Young's modulus of the elastic restraints that make the potential energy of the particle, that is, objective function, the global minimum constitute the solution of the problem. In the minimization process, a series of starting points for the design variables of Eq. (21) are selected at random from the region of interest. The lowest local minimum along the search trajectory initiated from each starting point is determined and recorded. A Bayesian argument is then used to establish the probability of the current overall minimum value of the objective function being the global minimum, given the number of starts and the number of times this value has been achieved. The multistart optimization procedure is terminated when a target probability, typically 0.99, has been exceeded.

#### IV. Experimental Investigation

In the experimental study, a number of laminated composite sandwich plates with different cores and face sheets were fabricated and subjected to impulse vibration testing. The dimensions ( $a_0 \times b_0 \times h$ ) of the laminated composite sandwich plates were  $30 \times 30 \times 0.375$  cm with a core thickness of 0.3 cm (core 1) or  $21 \times 30 \times 0.28$  cm with core thickness of 0.205 cm (core 2). The face sheets were fabricated using T300/2500 graphite/epoxy (Gr/ep) prepreg tapes produced by Torayca Co., Japan. The cores were made of foam (core 1) or plastics (core 2) materials. The elastic constants of the Gr/ep face sheets and cores were first determined experimentally using the standard specimens in accordance with ASTM standards D3039 and D695 [20]. In the material testing, each elastic constant was determined using three specimens. The means and coefficients of

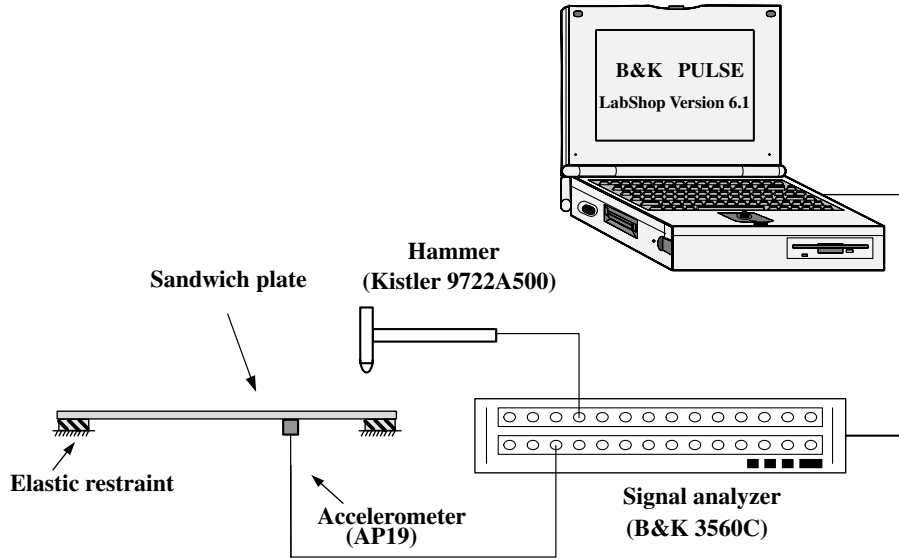


Fig. 5 Impulsive vibration testing of flexibly supported composite sandwich plate.

variation (COVs) of the elastic constants obtained from the tests are as follows:

Gr/ep face sheet

$$\begin{aligned} E_1 &= 146.503 \text{ GPa (0.72\%)}, & E_2 &= 9.223 \text{ GPa (1.19\%)} \\ G_{12} &= 6.836 \text{ GPa (3.16\%)} & \nu_{12} &= 0.306 (0.19\%) \\ h_f &= 0.375 \text{ mm} \end{aligned} \quad (25a)$$

Core

$$\begin{aligned} \text{core 1: } E_c &= 27.65 \text{ MPa (3.62\%)}, & \nu_c &= 0.3 (0.45\%), & h_c &= 3 \text{ mm} \\ \text{core 2: } E_c &= 3.94 \text{ GPa (2.58\%)}, & \nu_c &= 0.38 (0.31\%), & h_c &= 2.05 \text{ mm} \end{aligned} \quad (25b)$$

The values in the parentheses in the above equation denote the COVs of the elastic constants of the materials. The average mass densities of the core and face sheet of the  $30 \times 30$  cm sandwich plates were  $49.1$  and  $1675.4 \text{ kg/m}^3$ , respectively, whereas those of the  $21 \times 21$  cm sandwich plates were  $1244.1$  and  $1658.4 \text{ kg/m}^3$ , respectively. Strip-type pads made of foam plastic materials were used as the edge supports of the laminated composite sandwich plates. The elastic constant  $E_e$  of the flexible pads was also determined following the standard ASTM tensile testing procedure. The mean and COV of  $E_e$  were  $2.028 \text{ MPa}$  and  $2.3\%$ , respectively. The cross-sectional dimensions of the pads were  $b_e = 5$  and  $h_e = 2.1 \text{ mm}$ .

The laminated composite sandwich plates with elastically supported edges were subjected to the impulsive vibration testing as shown in Fig. 5. In the vibration testing of the composite sandwich plate, a hand held impulse hammer (Kistler 9722A500, Kistler Instrument, USA) was used to excite the composite sandwich plate at different points on the plate, a force transducer (Kistler 9904A, Kistler Instrument, USA) attached to the hammer's head to measure the input force, an accelerometer of mass  $0.14 \text{ g}$  (AP19, APTechnology, Netherland) to pick up the vibration response data at different locations on the plate, and a data acquisition and analysis system (B&K 3560C and B&K Pulse Labshop Version 6.1) to process the vibration data from which the natural frequencies of the composite plates were extracted. It is noted that for each pair of excitation and signal pickup points, the composite sandwich plate was tested several times. Each time when the plate was tested a set of vibration data was produced for constructing the frequency response spectrum of the plate from which the lower natural frequencies of the plates were extracted. A detailed study had shown that the small modal damping ratios with values less than  $2\%$  had negligible effects on the lower natural frequencies of the plates and the identified system parameters. Therefore without affecting the generality of the

present identification method, when determining the natural frequencies from the frequency response spectra, the frequencies associated with the peak responses were treated as the natural frequencies of the plates. For illustration purposes, Fig. 6 shows a typical frequency response spectrum of the square ( $30 \times 30 \text{ cm}$ )  $[0_3 \text{ deg / core } 1/0_3 \text{ deg}]$  plate with elastically restrained edges. It is noted that the first eight natural frequencies of the plate can be easily identified from the frequency response spectrum as shown in the figure. The means of the first eight measured natural frequencies of the flexibly supported laminated composite sandwich plates determined from the impulsive vibration testing of the plates are listed in Table 1. It is noted that the COVs of the natural frequencies obtained from the tests were less than  $1.1\%$ . For comparison purposes, the theoretical natural frequencies of the laminated composite sandwich plates determined using the experimental material constants of Eq. (25) in the present Rayleigh–Ritz method are also listed in Table 1. In the Rayleigh–Ritz analysis of the sandwich plates with flexible edges, the translational and rotational spring constant intensities in Eq. (10) were equal to  $K_L$  and  $K_R$ , respectively, given in Eq. (16). Furthermore because the plates were supported at their bottom surfaces, except the rotational spring constant intensity at the lower face sheet (layer group 3), all other rotational spring constant intensities were equal to 0. It is noted that the percentage differences between the experimental and theoretical natural frequencies of the sandwich plates were less than or equal to  $6.07\%$ . In the following system identification study, the measured natural frequencies of the sandwich plates in Table 1 will be used in solving the problem of Eq. (17) to demonstrate the applications of the proposed method.

## V. Results and Discussions

Before proceeding to the system parameters identification of laminated composite sandwich plates, a number of numerical examples are first given to illustrate the capability and accuracy of the proposed Raleigh–Ritz method in determining natural frequencies of laminated composite sandwich plates with different boundary conditions reported in the literature [21–23] or obtained via the use of the finite element code ANSYS [24]. A convergence study has shown that the uses of  $I = J = M = N = P = Q = 10$  for the characteristic functions in Eq. (12) are sufficient to make the solutions of the sandwich plates with different boundary conditions converge. Therefore from now on the aforementioned number of terms of the characteristic functions will be used in the Rayleigh–Ritz method for the following sandwich plate analyses. The results obtained by the present method are listed in Table 2 in comparison with those available in the literature or obtained in the finite element

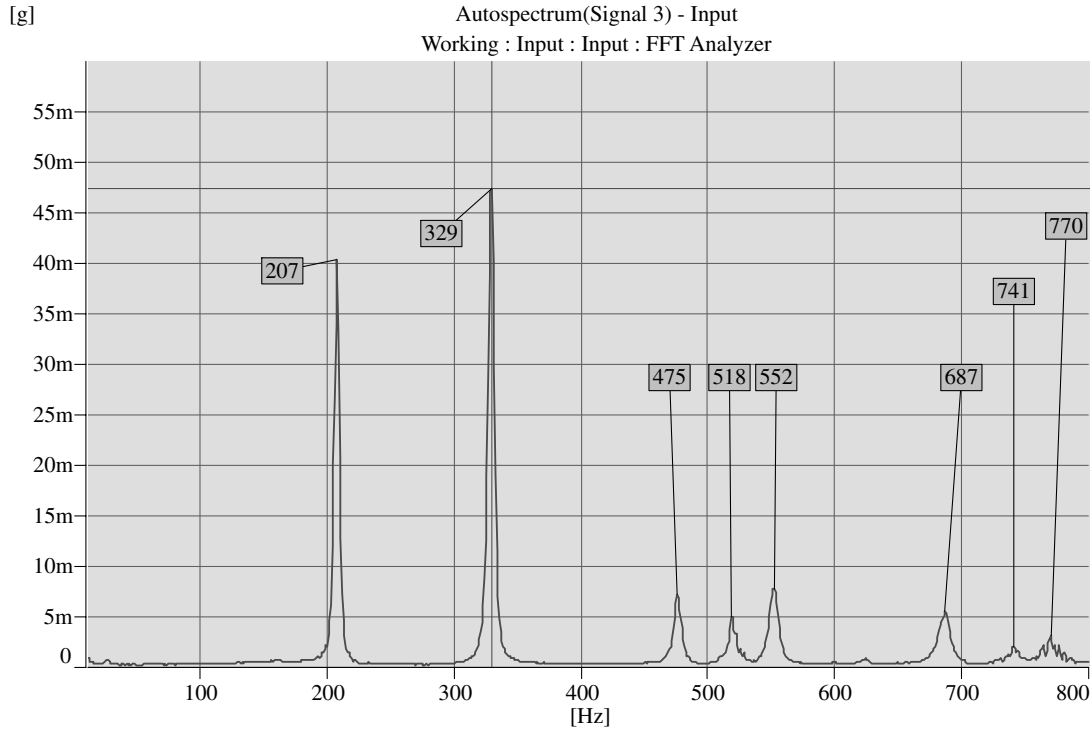


Fig. 6 Frequency response spectrum of the square  $[0_3 \text{ deg /core } 1/0_3 \text{ deg}]$  plate with elastic edge supporting pads.

analyses of the plates using the element type SHELL 91 of ANSYS. It is noted that in analyzing the sandwich plates with clamped edges, the translational spring constant intensity  $K_L$  is chosen as  $10^{10} \text{ N/m}^2$  whereas the rotational spring constant intensity  $K_R$  at all the layer groups is  $10^{10} \text{ N}$ . The results in Table 2 have shown that the present method can predict excellent natural frequencies for the laminated composite sandwich plates with simple supports. As for the sandwich plates with clamped edges, the present method can produce better results than the other methods when compared with the experimental results. The discrepancies between the experimental and theoretical natural frequencies for the clamped plates may be due to the imperfect clamping condition in which the edges of the plates were not perfectly clamped but rather restrained merely by elastic supports with relatively high stiffness. Therefore the actual boundary conditions should be modeled properly in the vibration formulation of the sandwich plates if more accurate prediction of the modal characteristics of the plates is desired. For the sandwich plates with

elastic supports, the present method can predict natural frequencies lower than those predicted by ANSYS. Next study the capability and accuracy of the present method for system parameters identification of laminated composite sandwich plates with different elastic restraints via a theoretical approach. The first eight theoretical (actual) natural frequencies of the flexibly supported  $[0_3 \text{ deg /core } 1/0_3 \text{ deg}]$  plate in Table 1 are treated as “measured” natural frequencies in the identification of the system parameters of the sandwich plate. The upper and lower bounds of the system parameters, which are reasonably large, are chosen based on experience.

$$\begin{aligned}
 0 \leq E_1 \leq 400 \text{ GPa}; & \quad 0 \leq E_2 \leq 40 \text{ GPa}; & \quad 0 \leq G_{12} \leq 20 \text{ GPa} \\
 0 \leq \nu_{12} \leq 0.5 & \quad 0 \leq E_c \leq 100 \text{ MPa}; & \quad 0 \leq \nu_c \leq 0.5 \\
 & \quad 0 \leq E_e \leq 10 \text{ MPa} & \quad (26)
 \end{aligned}$$

Table 1 Experimentally determined natural frequencies of flexibly supported laminated composite sandwich plates

Layup	Natural frequency, Hz							
	1st	2nd	3rd	4th	5th	6th	7th	8th
$[0_3 \text{ deg /core } 1/0_3 \text{ deg}]$	207 <sup>a</sup>	329	475	518	552	687	741	770
	208.63 <sup>b</sup>	326.04	476.68	533.05	548.92	698.86	749.19	781.67
	−0.78% <sup>c</sup>	0.91%	−0.35%	−2.82%	0.56%	−1.70%	−1.09%	−1.49%
$[0 \text{ deg /90 deg /0 deg /core } 1/0 \text{ deg /90 deg /0 deg}]$	227	439	501	635	704	724	819	838
	226.91	443.5	472.32	609.32	700.8	740.03	816.63	835.61
	0.04%	−1.01%	6.07%	4.21%	0.46%	−2.17%	0.29%	0.29%
$[0_3 \text{ deg /core } 2/0_3 \text{ deg}]$	263.5	407.4	694	761.9	842.8	1038.8	1082.8	1292.3
	257.15	398.72	677.55	737.63	816.56	1004.06	1053.43	1246.50
	2.47%	2.18%	2.43%	3.29%	3.21%	3.46%	2.79%	3.67%
$[0 \text{ deg /90 deg /0 deg /core } 2/0 \text{ deg /90 deg /0 deg}]$	273.9	614.8	713.8	920.5	1094.6	1223.3	1301.9	1361.5
	267.86	603.4	699.4	898.4	1076.55	1203	1074.95	1340.12
	2.25%	1.89%	2.06%	2.46%	1.68%	1.67%	2.11%	1.60%

<sup>a</sup>Experimental natural frequency.

<sup>b</sup>Theoretical natural frequency.

<sup>c</sup>Percentage difference.

**Table 2** Natural frequencies of laminated composite sandwich plates predicted by different methods

Layup	Edge support	Method	Natural frequency, Hz					
			1st	2nd	3rd	4th	5th	6th
[0 deg /core/0 deg]	Simply supported	Present	23.1	44.2	69.9	79.5	89.9	123.6
		Analytical [21]	23	44	71	80	91	126
		Experimental [21]	—	45	69	78	92	125
		Zhou and Li [22]	23.3	44.5	71.2	78.8	91.6	125.1
		Khare et al. [23]	23.5	45.0	72.5	80.6	93.4	128.2
		ANSYS	23.4	44.9	70.5	80.4	91.4	125.9
[30 <sub>3</sub> deg /core/30 <sub>3</sub> deg]	Clamped	Present	539.3	954.5	1164.2	1393.8	1758.6	1893.3
		Kanematsu et al. [25]	581	993	1131	1540	1759	—
		Experimental [25]	530	917	1138	1390	1620	—
		ANSYS	681.2	1106.7	1355.4	1564.6	1887.1	2071.2
[0 <sub>3</sub> deg /core/0 <sub>3</sub> deg]	Clamped	Present	560.6	907.6	1213.3	1454.7	1576.6	1983.5
		Kanematsu et al. [25]	567	1029	1155	1583	1768	—
		Experimental [25]	480	892	940	1356	1515	—
		ANSYS	667.2	1159.5	1287.0	1642.0	1897.0	2071.2
[0 deg /core/0 deg]	$K_L = 4 \times 10^6$ N/m <sup>2</sup>	Present <sup>a</sup>	665.0	1104.7	1567.6	1832.2	1846.0	2380.7
		ANSYS	673.1	1117.7	1596.3	1864.9	1873.2	2423.9
[45 deg /core/45 deg]	$K_R = 10$ N	Present	661.5	1209.6	1495.3	1727.9	2127.2	2312.5
		ANSYS	670.1	1227.1	1524.7	1754.9	2166.5	2351.8

<sup>a</sup>Material property and dimensions for the analysis. Face sheets:  $E_1/E_2 = 10$ ,  $G_{12}/E_2 = 0.6$ ,  $G_{23}/E_2 = 0.2$ ,  $\nu_{12} = 0.3$ ,  $E_2 = 10$  GPa,  $\rho_f = 1500$  kg/m<sup>3</sup>. Core:  $E_c = 100$  MPa,  $G_c = E_c/(2 + 2\nu_c)$ ,  $\nu_c = 0.3$ ,  $\rho_c = 50$  kg/m<sup>3</sup>;  $a = b = 0.205$  m,  $h_f = 0.125$  mm,  $h_c = 6.35$  mm.

The modified design variables of Eq. (21) when obtained via the use of the following normalization factors are less than 10.

$$\alpha_1 = \alpha_5 = 100$$

$$\alpha_4 = \alpha_6 = 1$$

and

$$\alpha_i = 10 \quad (i = 2, 3, 7) \quad (27)$$

Because the modified design variables are less than 10, the search for the solution can thus be expedited. In the identification process, 6 starting points are randomly generated and for each starting point around 20 ~ 30 iterations are required to locate the lowest local minimum. The starting points, the lowest local minima for the starting points, numbers of iterations required to obtain the lowest local minima, and the global minimum are listed in Table 3. It is noted that the actual system parameters have been identified in an efficient and effective way. Next consider the system identification of square [0<sub>3</sub> deg /core/0<sub>3</sub> deg] and [45 deg / - 45 deg /45 deg / core/45 deg / - 45 deg /45 deg] glass/epoxy (GI/ep) sandwich plates with lengths  $a = 21$  cm supported by elastic edge pads. The actual system parameters of the GI/ep sandwich plates are as follows.

$$E_1 = 38.6 \text{ GPa}, \quad E_2 = 8.27 \text{ GPa}, \quad G_{12} = 4.14 \text{ GPa}$$

$$\nu_{12} = 0.26, \quad \rho_f = 1800 \text{ kg/m}^3, \quad h_f = 0.375 \text{ mm}$$

$$E_c = 10 \quad \text{or} \quad 2000 \text{ MPa}; \quad \nu_c = 0.3$$

$$E_e = 1, \quad \text{or} \quad 50 \text{ MPa}, \quad \rho_c = 500 \text{ kg/m}^3, \quad h_c = 2 \text{ mm} \quad (28)$$

The actual natural frequencies of the GI/ep sandwich plates with different core properties supported by the elastic pads with different Young's moduli are listed in Table 4. Again the first eight actual natural frequencies, which are treated as the measured natural frequencies, are used in the present method to identify the system parameters of the GI/ep sandwich plates. The bounds of the system parameters, which are reasonably large, are chosen as the following.

$$0 \leq E_1 \leq 400 \text{ GPa}; \quad 0 \leq E_2 \leq 40 \text{ GPa}$$

$$0 \leq G_{12} \leq 20 \text{ GPa}; \quad 0 \leq \nu_{12} \leq 0.5 \quad 0 \leq E_c \leq 100 \text{ MPa}$$

$$0 \leq \nu_c \leq 0.5; \quad 0 \leq E_e \leq 10 \text{ MPa} \quad \text{for } E_c = 10 \text{ MPa}$$

$$0 \leq E_c \leq 10,000 \text{ MPa}; \quad 0 \leq \nu_c \leq 0.5$$

$$0 \leq E_e \leq 100 \text{ MPa} \quad \text{for } E_c = 2000 \text{ MPa} \quad (29)$$

**Table 3** Identified elastic constants of the flexibly supported Gr/ep [0<sub>3</sub> deg /core 1/0<sub>3</sub> deg] sandwich plate using actual natural frequencies

Starting point no.	Stage	System parameter							No. of iterations
		$E_1$ , GPa	$E_2$ , GPa	$G_{12}$ , GPa	$\nu_{12}$	$E_c$ , MPa	$\nu_c$	$E_e$ , MPa	
1	Initial	172.2333	1.7197	1.8401	0.3956	67.3468	0.4880	0.0487	23
	Final	146.5030	9.2230	6.8360	0.3060	27.6504	0.3000	2.0280	
2	Initial	219.5101	33.7476	8.3422	0.3833	83.8477	0.2117	1.0114	20
	Final	129.5830	8.1650	7.9054	0.4811	97.0487	0.3066	0.3368	
3	Initial	369.7264	19.4123	0.9951	0.2674	38.7409	0.1706	8.7940	30
	Final	146.5030	9.2230	6.8360	0.3060	27.6504	0.3000	2.0280	
4	Initial	14.6463	10.7449	4.9484	0.4198	50.1803	0.4227	0.2273	21
	Final	146.5030	9.2230	6.8360	0.3060	27.6503	0.3000	2.0280	
5	Initial	186.6666	13.7427	16.8817	0.1155	89.6623	0.3149	5.2605	20
	Final	146.5030	9.2230	6.8360	0.3060	27.6504	0.3000	2.0280	
6	Initial	294.1296	2.3754	1.5370	0.2186	80.2237	0.1777	9.3716	28
	Final	146.5030	9.2230	6.8360	0.3060	27.6504	0.3000	2.0280	
Global minimum		146.5030	9.2230	6.8360	0.3060	27.6503	0.3000	2.0280	Probability
		(0%) <sup>a</sup>	(0%)	(0%)	(0%)	(0.001%)	(0%)	(0%)	0.9959

<sup>a</sup>Values in the parentheses denote percentage difference between identified and actual data.

**Table 4** Actual natural frequencies of the Gl/ep plates supported by elastic restraints

Layup	Core $E_{\text{core}}$ , MPa	Edge support $E_e$ , MPa	Natural frequency, Hz							
			1st	2nd	3rd	4th	5th	6th	7th	8th
[0 <sub>3</sub> deg /core/0 <sub>3</sub> deg]	10	1	136.973	247.026	288.701	359.421	394.143	450.710	475.022	502.840
	2000	50	235.970	435.970	707.205	807.604	868.713	1188.530	1337.093	1469.987
[45 deg / - 45 deg /45 deg /core /45 deg / - 45 deg /45 deg]	10	1	144.680	275.273	281.788	376.092	428.958	433.161	499.676	511.431
	2000	50	261.519	578.494	621.462	965.500	1120.733	1154.065	1474.261	1581.640

The modified design variables of the Gl/ep sandwich plates when obtained via the use of the following normalization factors are less than 10.

$$\alpha_1 = 100 \quad \alpha_4 = \alpha_6 = 1 \quad \alpha_i = 10 \quad (i = 2, 3)$$

and

$$\begin{aligned} \alpha_5 &= 100, & \alpha_7 &= 10 & \text{for } E_c &= 10 \text{ MPa} \\ \alpha_5 &= 10,000, & \alpha_7 &= 100 & \text{for } E_c &= 2000 \text{ MPa} \end{aligned} \quad (30)$$

The numbers of starting points and the average numbers of iterations required to obtain the global minima for the cases are listed in Table 5. Again for all the cases under consideration, the actual system parameters of the Gl/ep sandwich plates can be determined in an efficient and effective way.

Now the present method is applied to the system identification of the laminated composite sandwich plates which have been tested. The first eight measured natural frequencies of the flexibly supported

[0<sub>3</sub> deg /core 1/0<sub>3</sub> deg] sandwich plate in Table 1 are used as an example to illustrate the system identification process of the present method. Table 6 lists the randomly generated starting points, the lowest local minima obtained for the starting points, the numbers of iterations required to get the lowest local minima, and the global minimum. It is noted that very good estimates of the system parameters with percentage differences less than or equal to 5.74% have been obtained for the [0<sub>3</sub> deg /core 1/0<sub>3</sub> deg] sandwich plate. For the other sandwich plates, the numbers of starting points, the average numbers of iterations, the identified system parameters, and the percentage differences between the actual and identified system parameters are listed in Table 7. In view of the identified system parameters listed in the table, it is noted that the percentage differences between the actual and identified system parameters for the sandwich plates are less than or equal to 12.51%. In general, among any set of the identified system parameters, only one of the system parameters may have a relatively large percentage difference, whereas those of the other identified system parameters are small. Though for engineering applications, percentage differences of material constants less than 15% have always been found to be acceptable, more in-depth investigation should be pursued to

**Table 5** System identification of flexibly supported Gl/ep sandwich plates using actual natural frequencies

Layup	Core $E_{\text{core}}$ , MPa	Edge support $E_e$ , MPa	No. of starting points	Average no. of iteration	System parameter						
					$E_1$ , GPa	$E_2$ , GPa	$G_{12}$ , GPa	$\nu_{12}$	$E_c$ , MPa	$\nu_c$	$E_e$ , MPa
[0 <sub>3</sub> deg /core/0 <sub>3</sub> deg]	10	1	6	11	38.6001	8.27	4.14	0.26	9.988	0.2985	1.0
	2000	50	4	13	(2.6e-4%) <sup>a</sup>	(0%)	(0%)	(0%)	(-0.12%)	(-0.5%)	(0%)
[45 deg / - 45 deg / 45 deg /core 45 deg / -45 deg /45 deg]	10	1	7	16	38.5964	8.2684	4.1391	0.26	2002.2	0.30	50.0004
					(-0.01%)	(-0.02%)	(-0.02%)	(0%)	(0.11%)	(0%)	(8e-4%)
	2000	50	4	13	38.6	8.27	4.14	0.26	9.99	0.2986	1.0
					(0%)	(0%)	(0%)	(0%)	(-0.1%)	(-0.47%)	(0%)
	2000	50	4	13	38.5951	8.2732	4.1403	0.2601	1999.6	0.30	50.0054
					(-0.01%)	(0.04%)	(0.01%)	(0.04%)	(-0.02%)	(0%)	(0.01%)

<sup>a</sup>Values in parentheses denote the percentage difference between identified and actual data.

**Table 6** Identified system parameters of the flexibly supported Gr/ep [0<sub>3</sub> deg /core 1/0<sub>3</sub> deg] sandwich plate using experimental natural frequencies

Starting point no.	Stage	System parameter							No. of iterations
		$E_1$ , GPa	$E_2$ , GPa	$G_{12}$ , GPa	$\nu_{12}$	$E_c$ , MPa	$\nu_c$	$E_e$ , MPa	
1	Initial	289.961	16.982	8.635	0.2205	49.983	0.3617	6.135	15
	Final	154.918	8.930	6.938	0.3003	26.933	0.3000	2.127	
2	Initial	194.668	18.840	1.202	0.1885	90.263	0.4001	2.056	20
	Final	154.920	8.930	6.938	0.3003	26.933	0.3000	2.127	
3	Initial	310.809	16.840	17.388	0.2859	10.782	0.1889	1.189	20
	Final	154.920	8.930	6.938	0.3003	26.933	0.3000	2.127	
4	Initial	15.501	35.283	0.169	0.3109	76.370	0.2995	2.180	16
	Final	154.911	8.930	6.937	0.3005	26.933	0.3000	2.127	
Global minimum		154.911	8.930	6.937	0.3005	26.933	0.3000	2.127	Probability
		(5.74%) <sup>a</sup>	(-3.18%)	(1.48%)	(-1.80%)	(-2.59%)	(0%)	(4.88%)	

<sup>a</sup>Values in the parentheses denote percentage difference between identified and measured data.



**Table 7** Identified system parameters of different flexibly supported laminated composite sandwich plates using measured natural frequencies

Layup	No. of starting points	Average no. of iteration	System parameter						
			$E_1$ , GPa	$E_2$ , GPa	$G_{12}$ , GPa	$\nu_{12}$	$E_c$ , MPa	$\nu_c$	$E_e$ , MPa
[0 deg /90 deg /0 deg /core 1 /0 deg /90 deg /0 deg]	4	28	151.162 (3.18%) <sup>a</sup>	8.121 (−11.95%)	7.540 (10.30%)	0.3200 (4.57%)	28.097 (1.62%)	0.2941 (−1.97%)	1.978 (−2.49%)
[0 <sub>3</sub> deg /core 2/0 <sub>3</sub> deg]	4	25	151.241 (3.23%)	9.203 (−0.22%)	6.756 (−1.17%)	0.3284 (7.33%)	4279.490 (8.62%)	0.3846 (1.21%)	2.230 (9.97%)
[0 deg /90 deg /0 deg /core 2 /0 deg /90 deg /0 deg]	6	18	157.930 (7.80%) <sup>a</sup>	8.599 (−6.77%)	6.559 (−4.06%)	0.3024 (−1.19%)	3447.275 (−12.51%)	0.3706 (−2.49%)	2.080 (2.54%)

<sup>a</sup>Values in the parentheses denote percentage difference between identified and measured data.

improve the accuracy of the identified system parameters in the future. Further study has shown that the use of over eight natural frequencies in the identification process will produce similar results. Finally it is worth pointing out that the differences between the identified and actual system parameters of the plates which have been tested in this study may be due to a number of uncertain factors including the use of an oversimplified model of the flexible supports, the effects of accelerometer mass on the plate vibration, and existence of noise in the measurement data. Regarding the modeling of the elastic edge pads, the mechanics of materials approach adopted to calculate the spring constants of the edge supports might be too simple to simulate the actual behaviors of the edge supports. Therefore a more sophisticated method such as the finite element method with the use of solid elements is needed to model the sandwich plate and its elastic edge supports if more accurate results are desired. The use of noncontact probes to measure plate vibration responses can eliminate the adverse effects of accelerometer mass imposed on plate vibration. On the other hand, the effects of the measurement noise on the identified system parameters and the sources of the noise should be studied in detail so that the measurement noise incurred in the vibration testing of the plates can be suppressed or the detrimental effects of the measurement noise be minimized or even eliminated.

## VI. Conclusions

A nondestructive evaluation method for system identification of laminated composite sandwich plates with elastic restraints using experimentally measured natural frequencies of the plates have been presented. The system identification process in the proposed method has included the use of the Rayleigh–Ritz method for predicting the theoretical natural frequencies of the laminated composite sandwich plates using trial values of the system parameters, the construction of the frequency discrepancy function that measures the sum of the

differences between the experimental and theoretical predictions of the system natural frequencies, the use of a multistart global minimization method to identify the elastic constants by making the frequency discrepancy function a global minimum, and a design variables normalization technique for expediting the convergence of the search of the global minimum. The accuracy of the present Rayleigh–Ritz method in predicting natural frequencies of laminated composite sandwich plates with different boundary conditions has been verified by the existing results reported in the literature. Both numerical and experimental investigations have been conducted to demonstrate the capability, effectiveness, accuracy, and applications of the proposed system identification method. In the theoretical study, it has been shown that the proposed method can identify the actual system parameters of elastically restrained laminated composite sandwich plates made of different laminated composite materials using the first eight natural frequencies in an efficient and effective way. In the experimental investigation, several flexibly restrained Gr/ep [0<sub>3</sub>/core 1/0<sub>3</sub> deg], [0 deg/90 deg/0 deg/core 1/0 deg/90 deg/0 deg], [0<sub>3</sub>/core 2/0<sub>3</sub> deg], and [0 deg/90 deg/0 deg/core 2/0 deg/90 deg/0 deg] sandwich plates with different core materials have been subjected to impulsive vibration testing to measure the lower natural frequencies of the plates. The uses of the first eight measured natural frequencies in the proposed method to identify the system parameters of the flexibly supported sandwich plates have also produced reasonably good estimates of the system parameters. The largest percentage difference between the actual and identified system parameter obtained in this study is 12.51% for core Young's modulus  $E_c$  whereas small percentage differences have been obtained for other system parameters. The factors that may cause the errors of the identified system parameters and several possible means for improving the accuracy of the identified system parameters have been proposed and discussed. The present identification method has the potential to be used as a preliminary technique for quick system parameters evaluation or structural integrity assessment.

## Appendix: Elements of System Matrices $K$ and $M$ of Symmetrically Laminated Composite Sandwich Plates with Elastically Restrained Edges

The eigenvalue problem of Eq. (15) is rewritten as

$$\begin{pmatrix} K^{11} & K^{12} & K^{13} & K^{14} & K^{15} & K^{16} & K^{17} \\ & K^{22} & K^{23} & K^{24} & K^{25} & K^{26} & K^{27} \\ & & K^{33} & K^{34} & K^{35} & K^{36} & K^{37} \\ & & & K^{44} & K^{45} & 0 & 0 \\ & & & & K^{55} & 0 & 0 \\ & & & & & K^{66} & K^{67} \\ & & & & & & K^{77} \end{pmatrix} - \omega^2 \begin{pmatrix} M^{11} & 0 & 0 & 0 & 0 & 0 & 0 \\ & M^{22} & 0 & M^{24} & 0 & M^{26} & 0 \\ & & M^{33} & 0 & M^{35} & 0 & M^{37} \\ & & & M^{44} & 0 & 0 & 0 \\ & & & & M^{55} & 0 & 0 \\ & & & & & M^{66} & 0 \\ & & & & & & M^{77} \end{pmatrix} \begin{pmatrix} C_{ij}^{(1)} \\ C_{mn}^{(2)} \\ C_{pq}^{(3)} \\ C_{m'n'}^{(4)} \\ C_{p'q'}^{(5)} \\ C_{m''n''}^{(6)} \\ C_{p''q''}^{(7)} \end{pmatrix} = \begin{pmatrix} 0 \\ 0 \\ 0 \\ 0 \\ 0 \\ 0 \\ 0 \end{pmatrix} \quad (A1)$$

where

$$\begin{aligned}
[K^{11}]_{ij\bar{j}} &= 4 \times \left[ (A_{44}^c + 2A_{44}^f) E_{ii}^{00} F_{jj}^{11} / b^2 \right. \\
&\quad + (A_{55}^c + 2A_{55}^f) E_{ii}^{11} F_{jj}^{00} / a^2 \\
&\quad + (A_{45}^c + 2A_{45}^f) (E_{ii}^{01} F_{jj}^{10} + E_{ii}^{10} F_{jj}^{01}) / (ab) \Big] \\
&\quad + 2 \times \left\{ F_{jj}^{00} [K_{L1} \phi_i(-1) \phi_{\bar{i}}(-1) + K_{L2} \phi_i(1) \phi_{\bar{i}}(1)] / a \right. \\
&\quad + E_{ii}^{00} [K_{L3} \phi_j(-1) \phi_{\bar{j}}(-1) + K_{L4} \phi_j(1) \phi_{\bar{j}}(1)] / b \Big\} \\
[K^{12}]_{ijmn} &= 2 \times (A_{45}^c E_{im}^{00} F_{jn}^{10} / b + A_{55}^c E_{im}^{10} F_{jn}^{00} / a) \\
[K^{13}]_{ijpq} &= 2 \times (A_{44}^c E_{ip}^{00} F_{jq}^{10} / b + A_{45}^c E_{ip}^{10} F_{jq}^{00} / a) \\
[K^{14}]_{ijm'n'} &= 2 \times (A_{45}^f E_{im'}^{00} F_{jn'}^{10} / b + A_{55}^f E_{im'}^{10} F_{jn'}^{00} / a) \\
[K^{15}]_{ijp'q'} &= 2 \times (A_{44}^f E_{ip'}^{00} F_{jq'}^{10} / b + A_{45}^f E_{ip'}^{10} F_{jq'}^{00} / a) \\
[K^{16}]_{ijm''n''} &= 2 \times (A_{45}^f E_{im''}^{00} F_{jn''}^{10} / b + A_{55}^f E_{im''}^{10} F_{jn''}^{00} / a) \\
[K^{17}]_{ijp''q''} &= 2 \times (A_{44}^f E_{ip''}^{00} F_{jq''}^{10} / b + A_{45}^f E_{ip''}^{10} F_{jq''}^{00} / a) \\
[K^{22}]_{mn\bar{m}\bar{n}} &= A_{55}^c E_{m\bar{m}}^{00} F_{n\bar{n}}^{00} + (4D_{11}^c + 2A_{11}^f \times h_c^2) \times E_{m\bar{m}}^{11} F_{n\bar{n}}^{00} / a^2 \\
&\quad + (4D_{13}^c + 2A_{13}^f \times h_c^2) (E_{m\bar{m}}^{01} F_{n\bar{n}}^{10} + E_{m\bar{m}}^{10} F_{n\bar{n}}^{01}) / (ab) \\
&\quad + (4D_{33}^c + 2A_{33}^f \times h_c^2) \times E_{m\bar{m}}^{00} F_{n\bar{n}}^{11} / b^2 \\
&\quad + 2 \times F_{n\bar{n}}^{00} [K_{R1}^{(1)} \phi_m(-1) \phi_{\bar{m}}(-1) + K_{R2}^{(1)} \phi_m(1) \phi_{\bar{m}}(1)] / a \\
[K^{23}]_{mnpq} &= A_{45}^c E_{mp}^{00} F_{nq}^{00} + (4D_{13}^c + 2A_{13}^f \times h_c^2) E_{mp}^{11} F_{nq}^{00} / a^2 \\
&\quad + \left[ (4D_{12}^c + 2A_{12}^f \times h_c^2) E_{mp}^{10} F_{nq}^{01} \right. \\
&\quad + (4D_{33}^c + 2A_{33}^f \times h_c^2) E_{mp}^{01} F_{nq}^{10} \Big] / (ab) \\
&\quad + (4D_{23}^c + 2A_{23}^f \times h_c^2) E_{mp}^{00} F_{nq}^{11} / b^2 \\
[K^{24}]_{mm'm'n'} &= 2h_c \times \left[ B_{11}^f E_{mm'}^{11} F_{nn'}^{00} / a^2 + B_{33}^f E_{mm'}^{00} F_{nn'}^{11} / b^2 \right. \\
&\quad + B_{13}^f (E_{mm'}^{10} F_{nn'}^{01} + E_{mm'}^{01} F_{nn'}^{10}) / (ab) \Big] \\
[K^{25}]_{mnp'q'} &= 2h_c \times \left[ B_{13}^f E_{mp'}^{11} F_{nq'}^{00} / a^2 + B_{23}^f E_{mp'}^{00} F_{nq'}^{11} / b^2 \right. \\
&\quad + (B_{12}^f E_{mp'}^{10} F_{nq'}^{01} + B_{33}^f E_{mp'}^{01} F_{nq'}^{10}) / (ab) \Big] \\
[K^{26}]_{mmn''n''} &= 2h_c \times \left[ B_{11}^f E_{mm''}^{11} F_{nn''}^{00} / a^2 + B_{33}^f E_{mm''}^{00} F_{nn''}^{11} / b^2 \right. \\
&\quad + B_{13}^f (E_{mm''}^{10} F_{nn''}^{01} + E_{mm''}^{01} F_{nn''}^{10}) / (ab) \Big] \\
[K^{27}]_{mnp''q''} &= 2h_c \times \left[ B_{13}^f E_{mp''}^{11} F_{nq''}^{00} / a^2 + B_{23}^f E_{mp''}^{00} F_{nq''}^{11} / b^2 \right. \\
&\quad + (B_{12}^f E_{mp''}^{10} F_{nq''}^{01} + B_{33}^f E_{mp''}^{01} F_{nq''}^{10}) / (ab) \Big]
\end{aligned}$$

$$\begin{aligned}
[K^{33}]_{pq\bar{p}\bar{q}} &= A_{44}^c E_{p\bar{p}}^{00} F_{q\bar{q}}^{00} + (4D_{33}^c + 2A_{33}^f \times h_c^2) E_{p\bar{p}}^{11} F_{q\bar{q}}^{00} / a^2 \\
&\quad + (4D_{22}^c + 2A_{22}^f \times h_c^2) E_{p\bar{p}}^{00} F_{q\bar{q}}^{11} / b^2 \\
&\quad + (4D_{23}^c + 2A_{23}^f \times h_c^2) (E_{p\bar{p}}^{10} F_{q\bar{q}}^{01} + E_{p\bar{p}}^{01} F_{q\bar{q}}^{10}) / (ab) \\
&\quad + 2 \times E_{p\bar{p}}^{00} [K_{R3}^{(1)} \varphi_q(-1) \varphi_{\bar{q}}(-1) + K_{R4}^{(1)} \varphi_q(1) \varphi_{\bar{q}}(1)] / b \\
[K^{34}]_{pqm'n'} &= 2h_c \times \left[ B_{13}^f E_{pm'}^{11} F_{qn'}^{00} / a^2 + B_{23}^f E_{pm'}^{00} F_{qn'}^{11} / b^2 \right. \\
&\quad + (B_{33}^f E_{pm'}^{10} F_{qn'}^{01} + B_{12}^f E_{pm'}^{01} F_{qn'}^{10}) / (ab) \Big] \\
[K^{35}]_{pqp'q'} &= 2h_c \times \left[ B_{33}^f E_{pp'}^{11} F_{qq'}^{00} / a^2 + B_{22}^f E_{pp'}^{00} F_{qq'}^{11} / b^2 \right. \\
&\quad + B_{23}^f (E_{pp'}^{10} F_{qq'}^{01} + E_{pp'}^{01} F_{qq'}^{10}) / (ab) \Big] \\
[K^{36}]_{pqm''n''} &= 2h_c \times \left[ B_{13}^f E_{pm''}^{11} F_{qn''}^{00} / a^2 + B_{23}^f E_{pm''}^{00} F_{qn''}^{11} / b^2 \right. \\
&\quad + (B_{33}^f E_{pm''}^{10} F_{qn''}^{01} + B_{12}^f E_{pm''}^{01} F_{qn''}^{10}) / (ab) \Big] \\
[K^{37}]_{pqp''q''} &= 2h_c \times \left[ B_{33}^f E_{pp''}^{11} F_{qq''}^{00} / a^2 + B_{22}^f E_{pp''}^{00} F_{qq''}^{11} / b^2 \right. \\
&\quad + B_{23}^f (E_{pp''}^{10} F_{qq''}^{01} + E_{pp''}^{01} F_{qq''}^{10}) / (ab) \Big] \\
[K^{44}]_{m'n'\bar{m}'\bar{n}'} &= A_{55}^f E_{m\bar{m}'}^{00} F_{n\bar{n}'}^{00} + 4 \times \left[ D_{11}^f E_{m\bar{m}'}^{11} F_{n\bar{n}'}^{00} / a^2 \right. \\
&\quad + D_{33}^f E_{m\bar{m}'}^{00} F_{n\bar{n}'}^{11} / b^2 + D_{13}^f (E_{m\bar{m}'}^{10} F_{n\bar{n}'}^{01} + E_{m\bar{m}'}^{01} F_{n\bar{n}'}^{10}) / (ab) \Big] \\
&\quad + 2 \times F_{n\bar{n}'}^{00} [K_{R1}^{(2)} \phi_{m'}(-1) \phi_{\bar{m}'}(-1) + K_{R2}^{(2)} \phi_{m'}(1) \phi_{\bar{m}'}(1)] / a \\
[K^{45}]_{m'n'p'q'} &= A_{45}^f E_{m'p'}^{00} F_{n'q'}^{00} + 4 \times \left[ D_{13}^f E_{m'p'}^{11} F_{n'q'}^{00} / a^2 \right. \\
&\quad + D_{23}^f E_{m'p'}^{00} F_{n'q'}^{11} / b^2 + (D_{12}^f E_{m'p'}^{10} F_{n'q'}^{01} + D_{33}^f E_{m'p'}^{01} F_{n'q'}^{10}) / (ab) \Big] \\
[K^{55}]_{p'q'\bar{p}'\bar{q}'} &= A_{44}^f E_{p'\bar{p}'}^{00} F_{q'\bar{q}'}^{00} + 4 \times \left[ D_{33}^f E_{p'\bar{p}'}^{11} F_{q'\bar{q}'}^{00} / a^2 \right. \\
&\quad + D_{22}^f E_{p'\bar{p}'}^{00} F_{q'\bar{q}'}^{11} / b^2 + D_{23}^f (E_{p'\bar{p}'}^{10} F_{q'\bar{q}'}^{01} + E_{p'\bar{p}'}^{01} F_{q'\bar{q}'}^{10}) / (ab) \Big] \\
&\quad + 2 \times E_{p'\bar{p}'}^{00} [K_{R3}^{(2)} \varphi_{q'}(-1) \varphi_{\bar{q}'}(-1) + K_{R4}^{(2)} \varphi_{q'}(1) \varphi_{\bar{q}'}(1)] / b \\
[K^{66}]_{m''n''\bar{m}''\bar{n}''} &= A_{55}^f E_{m''\bar{m}''}^{00} F_{n''\bar{n}''}^{00} + 4 \times \left[ D_{11}^f E_{m''\bar{m}''}^{11} F_{n''\bar{n}''}^{00} / a^2 \right. \\
&\quad + D_{33}^f E_{m''\bar{m}''}^{00} F_{n''\bar{n}''}^{11} / b^2 + D_{13}^f (E_{m''\bar{m}''}^{10} F_{n''\bar{n}''}^{01} + E_{m''\bar{m}''}^{01} F_{n''\bar{n}''}^{10}) / (ab) \Big] \\
&\quad + 2 \times F_{n''\bar{n}''}^{00} [K_{R1}^{(3)} \phi_{m''}(-1) \phi_{\bar{m}''}(-1) + K_{R2}^{(3)} \phi_{m''}(1) \phi_{\bar{m}''}(1)] / a \\
[K^{67}]_{m''n''p''q''} &= A_{45}^f E_{m''p''}^{00} F_{n''q''}^{00} + 4 \times \left[ D_{13}^f E_{m''p''}^{11} F_{n''q''}^{00} / a^2 \right. \\
&\quad + D_{23}^f E_{m''p''}^{00} F_{n''q''}^{11} / b^2 + (D_{12}^f E_{m''p''}^{10} F_{n''q''}^{01} + D_{33}^f E_{m''p''}^{01} F_{n''q''}^{10}) / (ab) \Big] \\
[K^{77}]_{p''q''\bar{p}''\bar{q}''} &= A_{44}^f E_{p''\bar{p}''}^{00} F_{q''\bar{q}''}^{00} + 4 \times \left[ D_{33}^f E_{p''\bar{p}''}^{11} F_{q''\bar{q}''}^{00} / a^2 \right. \\
&\quad + D_{22}^f E_{p''\bar{p}''}^{00} F_{q''\bar{q}''}^{11} / b^2 + D_{23}^f (E_{p''\bar{p}''}^{10} F_{q''\bar{q}''}^{01} + E_{p''\bar{p}''}^{01} F_{q''\bar{q}''}^{10}) / (ab) \Big] \\
&\quad + 2 \times E_{p''\bar{p}''}^{00} [K_{R3}^{(3)} \varphi_{q''}(-1) \varphi_{\bar{q}''}(-1) + K_{R4}^{(3)} \varphi_{q''}(1) \varphi_{\bar{q}''}(1)] / b
\end{aligned}$$

$$[M^{11}]_{i\bar{j}\bar{j}} = (\rho_c h_c + 2\rho_f h_f) E_{ii}^{00} F_{j\bar{j}}^{00}$$

$$[M^{22}]_{mn\bar{m}\bar{n}} = \left( \rho_c h_c^3/12 + \rho_f h_c^2 h_f/2 \right) E_{mn}^{00} F_{\bar{m}\bar{n}}^{00}$$

$$[M^{24}]_{mn\bar{m}'n'} = \rho_f h_c h_f^2 \times E_{mn}^{00} F_{n'n'}^{00}/4$$

$$[M^{26}]_{mn\bar{m}''n''} = \rho_f h_c h_f^2 \times E_{mn}^{00} F_{n''n''}^{00}/4$$

$$[M^{33}]_{pq\bar{p}\bar{q}} = \left( \rho_c h_c^3/12 + \rho_f h_c^2 h_f/2 \right) E_{p\bar{p}}^{00} F_{q\bar{q}}^{00}$$

$$[M^{35}]_{pq\bar{p}'q'} = \rho_f h_c h_f^2 \times E_{p\bar{p}'}^{00} F_{q'q'}^{00}/4$$

$$[M^{37}]_{pq\bar{p}''q''} = \rho_f h_c h_f^2 \times E_{p\bar{p}''}^{00} F_{q''q''}^{00}/4$$

$$[M^{44}]_{m'n'\bar{m}'\bar{n}'} = \rho_f h_f^3 \times E_{m'\bar{m}'}^{00} F_{n'\bar{n}'}^{00}/3$$

$$[M^{55}]_{p'q'\bar{p}'\bar{q}'} = \rho_f h_f^3 \times E_{p'\bar{p}'}^{00} F_{q'\bar{q}'}^{00}/3$$

$$[M^{66}]_{m''n''\bar{m}''\bar{n}''} = \rho_f h_f^3 \times E_{m''\bar{m}''}^{00} F_{n''\bar{n}''}^{00}/3$$

$$[M^{77}]_{p''q''\bar{p}''\bar{q}''} = \rho_f h_f^3 \times E_{p''\bar{p}''}^{00} F_{q''\bar{q}''}^{00}/3$$

$$r, s = 0, 1; \quad i, j, \bar{i}, \bar{j}, i', j', \bar{i}', \bar{j}' = 1, 2, 3, \dots, I, J$$

$$m, n, \bar{m}, \bar{n}, m', n', \bar{m}', \bar{n}', m'', n'', \bar{m}'', \bar{n}'' = 1, 2, 3, \dots, M, N$$

$$p, q, \bar{p}, \bar{q}, p', q', \bar{p}', \bar{q}', p'', q'', \bar{p}'', \bar{q}'' = 1, 2, 3, \dots, P, Q$$

with

$$E_{im}^{rs} = \int_{-1}^1 \left[ \frac{d^r \phi_i(\xi)}{d\xi^r} \frac{d^s \phi_m(\xi)}{d\xi^s} \right] d\xi;$$

$$F_{jn}^{rs} = \int_{-1}^1 \left[ \frac{d^r \varphi_j(\eta)}{d\eta^r} \frac{d^s \varphi_n(\eta)}{d\eta^s} \right] d\eta$$

and the components of in-plane stiffness  $A_{ij}^c = A_{ij}^{(1)}$ ,  $A_{ij}^f = A_{ij}^{(2)} = A_{ij}^{(3)}$ ; bending-stretching coupling stiffness  $B_{ij}^c = B_{ij}^{(1)} = 0$ ,  $B_{ij}^f = B_{ij}^{(2)} = -B_{ij}^{(3)}$ ; and bending stiffness  $D_{ij}^c = D_{ij}^{(1)}$ ,  $D_{ij}^f = D_{ij}^{(2)} = D_{ij}^{(3)}$ .

### Acknowledgment

This research work was supported by the National Science Council of the Republic of China under Grant No. NSC 94-2212-E-009-020. Its support is gratefully appreciated.

### References

- [1] Deobald, L. R., and Gibbon, R. F., "Determination of Elastic Constants of Orthotropic Plates by a Modal Analysis/Rayleigh-Ritz Technique," *Journal of Sound and Vibration*, Vol. 124, No. 2, 1988, pp. 269–283.
- [2] Castagnède, B., Jenkins, J. T., Sachse, W., and Baste, S., "Optimal Determination of the Elastic Constants of Composite Materials from Ultrasonic Wave-Speed Measurements," *Journal of Applied Physics*, Vol. 67, No. 6, 1990, pp. 2753–2761.
- [3] Fallstrom, K. E., and Jonsson, M., "A Nondestructive Method to Determine Material Properties in Anisotropic Plate," *Polymer Composites*, Vol. 12, No. 5, 1991, pp. 293–305.
- [4] Berman, A., and Nagy, E. J., "Improvement of a Large Analytical Model Using Test Data," *AIAA Journal*, Vol. 21, No. 8, 1983, pp. 1168–1173.
- [5] Kam, T. Y., and Lee, T. Y., "Crack Size Identification Using an Expanded Mode Method," *International Journal of Solids and Structures*, Vol. 31, No. 7, 1994, pp. 925–940.
- [6] Kam, T. Y., and Liu, C. K., "Stiffness Identification of Laminated Composite Shafts," *International Journal of Mechanical Sciences*, Vol. 40, No. 9, 1998, pp. 927–936.
- [7] Wang, W. T., and Kam, T. Y., "Elastic Constants Identification of Shear Deformable Laminated Composite Plates," *Journal of Engineering Mechanics*, Vol. 127, No. 11, 2001, pp. 1117–1123.
- [8] Moussu, F., and Nivoit, M., "Determination of Elastic Constants of Orthotropic Plates by a Modal Analysis/Method of Superposition," *Journal of Sound and Vibration*, Vol. 165, No. 1, 1993, pp. 149–163.
- [9] Sol, H., Hua, J., Visscher, J., Vantomme, J., and Wilde, W. P., "A Mixed Numerical/Experimental Technique for the Nondestructive Identification of the Stiffness Properties of Fibre Reinforced Composite Materials," *NDT and E International*, Vol. 30, No. 2, 1997, pp. 85–91.
- [10] Qian, G. L., Hoa, S. V., and Xiao, X., "A Vibration Method for Measuring Mechanical Properties of Composite, Theory and Experiment," *Journal of Composite Structures*, Vol. 39, Nos. 1–2, 1997, pp. 31–38.
- [11] Hwang, S. F., and Chang, C. S., "Determination of Elastic Constants of Materials by Vibration Testing," *Journal of Composite Structures*, Vol. 49, No. 2, 2000, pp. 183–190.
- [12] Thwaites, S., and Clark, N. H., "Nondestructive Testing of Honeycomb Sandwich Structures Using Elastic Waves," *Journal of Sound and Vibration*, Vol. 187, No. 2, 1995, pp. 253–269.
- [13] Saito, T., Parbery, R. D., Okuno, S., and Kawano, S., "Parameter Identification for Aluminum Honeycomb Sandwich Panels Based on Orthotropic Timoshenko Beam Theory," *Journal of Sound and Vibration*, Vol. 208, No. 2, 1997, pp. 271–287.
- [14] Lee, C. R., and Kam, T. Y., "System Identification of Partially Restrained Composite Plates Using Measured Natural Frequencies," *Journal of Engineering Mechanics* (to be published).
- [15] Mau, S. T., "A Refined Laminated Plate Theory," *Journal of Applied Mechanics*, Vol. 40, June 1973, pp. 606–607.
- [16] Kam, T. Y., and Jan, T. P., "First-Ply Failure Analysis of Laminated Composite Plates Based on the Layerwise Linear Displacement Theory," *Journal of Composite Structures*, Vol. 32, No. 4, 1995, pp. 583–591.
- [17] Swanson, S. R., *Introduction to Design and Analysis with Advanced Composite Materials*, Prentice-Hall, Upper Saddle River, NJ, 1997, p. 36.
- [18] Vanderplaats, G. N., *Numerical Optimization Techniques for Engineering Design with Applications*, McGraw-Hill, New York, 1984, Chap. 5.
- [19] Snyman, J. A., and Fatti, L. P., "A Multistart Global Minimization Algorithm with Dynamic Search Trajectories," *Journal of Optimization Theory and Applications*, Vol. 54, No. 1, 1987, pp. 121–141.
- [20] ASTM Committee (ed.), *ASTM Standards and Literature References for Composite Materials*, 2nd ed., American Society for Testing and Materials, West Conshohocken, PA, 1990.
- [21] Raville, M. E., and Ueng, C. E. S., "Determination of Natural Frequencies of Vibration of a Sandwich Plate," *Experimental Mechanics*, Vol. 7, No. 11, 1967, pp. 490–493.
- [22] Zhou, H. B., and Li, G. Y., "Free Vibration Analysis of Sandwich Plates with Laminated Faces Using Spline Finite Point Method," *Computers and Structures*, Vol. 59, No. 2, 1996, pp. 257–263.
- [23] Khare, R. K., Kant, T., and Garg, A. K., "Free Vibration of Composite and Sandwich Laminates with a Higher-Order Facet Shell Element," *Composite Structures*, Vol. 65, Nos. 3–4, 2004, pp. 405–418.
- [24] Kohnke, P., *The ANSYS User's Manual*, Swanson Analysis System, Inc., Houston, PA, 1995.
- [25] Kanematsuo, H. H., Hirano, Y., and Iyama, H., "Bending and Vibration Of CFRP-Faced Rectangular Sandwich Plates," *Composite Structures*, Vol. 10, No. 2, 1988, pp. 145–163.

M. Hyer  
Associate Editor